ELSEVIER

Thermochimica Acta 346 (2000) 169–175

thermochimica acta

www.elsevier.com/locate/tca

Thermal and spectroscopic studies on the decomposition of [Ni{di(2-aminoethyl)amine}$_2$]- and [Ni(2,2′:6′,2″-terpyridine)$_2$]-Montmorillonite intercalated composites

Moushumi Bora[a], Jatindra Nath Ganguli[a,b], Dipak Kumar Dutta[a,*]

[a]*Material Science Division, Regional Research Laboratory (CSIR), Jorhat 785006, Assam, India*
[b]*Department of Chemistry, Guwahati University, Guwahati 781014, Assam, India*

Received 16 August 1999; received in revised form 23 November 1999; accepted 25 November 1999

Abstract

Intercalated [Ni{di(2-aminoethyl)amine}$_2$]-Montmorillonite (**I**) and [Ni(2,2′:6′,2″-terpyridine)$_2$]-Montmorillonite (**II**) composites have been synthesized and their thermal behavior studied by TG, DTG and DTA substantiated by XRD and IR spectroscopy. Thermal stabilities of the composites **I** and **II** were about 50 and 150°C higher, respectively, compared to their respective free metal complex salts. These results indicate that the metal complex with aromatic backboned ligands had higher thermal stability than that of the aliphatic one upon intercalation into layered clay. XRD data showed that on heating, the basal spacing (d_{001}) of the **I** composite decreased gradually from 14.5 Å at 50°C to about 13.5 Å at 250°C which may correspond with the transformation to a distorted octahedral metal complex in the interlamellar spacing of the clay. On the other hand, the **II** composite showed a basal spacing (d_{001}) of about 19.4 Å at 50°C, which decreased slightly to 19.0 Å at about 350°C indicating the presence of intercalated octahedral metal complex and thus corroborates the thermal analyses. IR spectra show characteristic bands of **I** and **II** composites up to about 250 and 350°C, respectively, which also support the data of thermal as well as XRD analyses. Such metal–complex–clay composites may be utilized for developing microporous layered materials exhibiting comparatively higher thermal stability.

Keywords: Intercalation; Interlamellar; Basal spacing; [Ni{di(2-aminoethyl)amine}$_2$]-Montmorillonite; [Ni(2,2′:6′,2″-terpyridine)$_2$]-Montmorillonite composites

1. Introduction

Incorporation of organic or inorganic cationic compounds into layered structures like Montmorillonite (Mnt) clay can result in microporous materials having definite gallery height depending upon the size and shape of the cations [1–8]. Organic cations like tetraalkylammonium ions are intercalated into smectites during the preparation of chromatographic materials for separation of mixtures of gases [9–13]. But the organo-Mnt clay composites, in general, exhibit limited thermal stability due to decomposition of the organic moiety at comparatively low temperature (<200°C) [14] and hence these composites may not be useful in systems where a comparatively higher temperature (>200°C) is involved. On the other hand, metal complexes containing suitable organic ligands exhibit comparatively higher thermal stability which

* Corresponding author. Tel.: +91-376-370012; fax: +91-376-370011.
E-mail address: pkbarooa@csir.res.in (D.K. Dutta).

0040-6031/00/$ – see front matter
PII: S0040-6031(99)00410-4

is further enhanced upon intercalation into Mnt [15–17]. Therefore, suitable metal complexes may be superior to cationic organic molecules as intercalating species in developing microporous Mnt clay composites with higher thermal stability. The aim of the present work is to investigate the intercalation of two bulky three-dimensional cationic metal-complexes, i.e., $[Ni(den)_2]Cl_2$ and $[Ni(tpy)_2](ClO_4)_2$ (where den=di(2-aminoethyl) amine and tpy=2,2′:6′,2″-terpyridine) with Na-Mnt and to evaluate the thermal stability of the intercalated products by thermogravimetry (TG), differential thermogravimetry (DTG) and differential thermal analysis (DTA) supplemented by X-ray diffraction (XRD) and infrared (IR) spectroscopy.

2. Experimental

2.1. Materials and methods

Montmorillonite clay, collected from M/S Neelkanth Sodaclays and Pulverisers, Jodhpur, India, contained silica sand, iron oxide etc. as impurities, and was purified by the sedimentation method [18]. The <2 μm fraction was collected. The oxide composition of the clay was SiO_2: 49.42; Al_2O_3: 20.02; Fe_2O_3: 7.43; TiO_2: 1.55; CaO: 0.69; MgO: 2.82; Na_2O: 0.09; LOI: 17.91 and others 0.07%. The clay was converted to the Na-exchanged form by stirring in 2 M NaCl solution for about 78 h and then washed and finally dialyzed against distilled water until the conductivity of the dialyzate approached that of distilled water. Ni-Mnt was prepared by treating Na-Mnt with 2 M $NiCl_2$ solution by following the same procedure as above. The cation exchange capacity (CEC) of the clay was found [19] to be 114 milli equivalent/100 g of clay. The complex $Ni(den)_2]Cl_2$ was prepared by the standard method reported in [20] and the complex $[Ni(tpy)_2](ClO_4)_2$ was a gift [21]. About 25 mg of Na-Mnt was suspended in about 10 ml of water by ultrasonication for 10 min and to it 10 ml solution containing 4.6 mg (55.6 mmol per 100 g clay) of $[Ni(den)_2]Cl_2$ complex was added. The whole mixture was stirred for 30 min. Similarly, 25 mg of Na-Mnt was intercalated with a solution of $[Ni(tpy)_2](ClO_4)_2$ containing 10.5 mg (56.6 mmol per 100 g clay) of the complex. The intercalation reaction between the metal complexes and Na-Mnt may be presented as:

$$\text{Na-Mnt} + [Ni(L)_2]^{2+} \rightarrow \underset{\text{(Where L=den, tpy)}}{[Ni(L)_2]\text{-Mnt}} + Na^+ \quad (1)$$

The adsorption of the metal complex by the clay was monitored by a UV–VIS spectrophotometer (Shimadzu, UV-160A, Japan). After completion of the intercalation reaction, the products were purified by washing 3 to 4 times with about 30 ml of distilled water and then dried at 50±5°C in an air oven. Elemental (C, H and N) analyses of the dried samples were also carried out (Perkin–Elmer, Model 2400). The results indicated that metal complexes were adsorbed by Mnt clay up to about 57 mmol per 100 g clay. TG, DTG and DTA were carried out with the Thermal analysers (Shimadzu Model 30-H, Kyota, Japan and TA-instruments, Model SDT 2960 Simultaneous DTA-DTG) at a heating rate at 20°C min^{-1} in an air atmosphere. Oriented samples were prepared on glass slides by standard techniques [22] and dried at room temperature, 100, 150, 200, 250, 300, 350 and 400°C for about 1 h for XRD study. XRD patterns were taken in the range 2θ=2–60° at a rate of 6°/min (X-ray Diffractometer Jeol, JDX-11p3A, Japan) using Cu Kα radiation. FT-IR spectra were obtained from KBr (Analytical grade and dried at 110°C) pressed discs of about 12 mm diameter and 1 mm thickness prepared by applying about 8×10^3 bar pressure for 10 min on finely ground particles containing about 3 mg material and 97 mg KBr in the range 400–4000 cm^{-1} using a Perkin–Elmer Infrared Spectrophotometer, Model 580 B.

3. Results and discussion

3.1. DTA, TG and DTG studies

The DTA–TG–DTG curves of Na- and Ni-Mnt are shown in Fig. 1. Na- and Ni-Mnt each shows the first and second endothermic peaks in the DTA curve in the temperature ranges 50–150°C and 480–520°C. These correspond to dehydration from the interlayer water and dehydroxylation of the clay, respectively. The TG and DTG curves show two mass loss stages. In the first stage up to about 150°C, Na- and Ni-Mnt show mass loss of about 14 and 17%, respectively, and correspond to loss of water from the interlayer spacing [23,24]. In the second stage, Na- and Ni-Mnt exhibit mass loss of

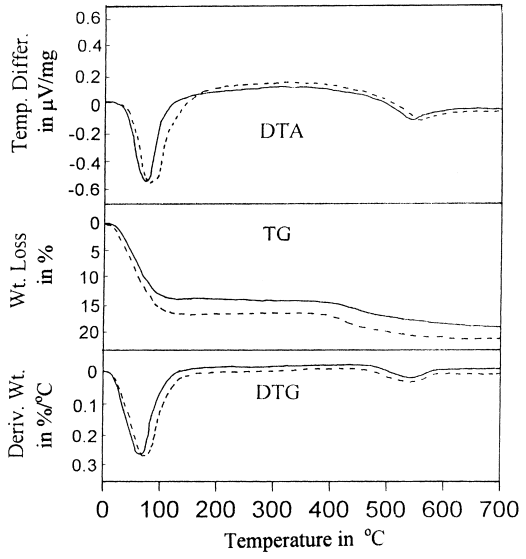

Fig. 1. TG–DTG–DTA curves of (a) Solid lines — Na-Mnt and (b) Dashed lines — Ni-Mnt.

about 3.8 and 4.5%, respectively, in the temperature range 480–520°C, and is attributed to loss of OH lattice water of the clay [23]. The DTA–TG–DTG curves of [Ni(den)$_2$]-Mnt composite are shown in Fig. 2. The DTA curve shows five peaks and the TG curve exhibits three mass loss stages. The first DTA curve shows a very broad endotherm from 75 to

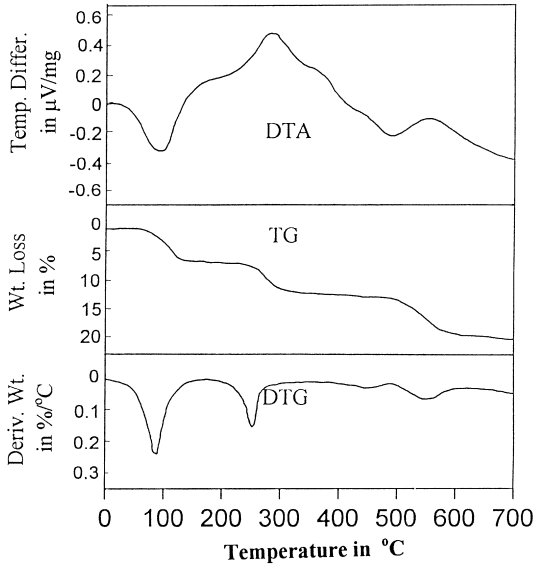

Fig. 2. TG–DTG–DTA curves of [Ni(den)$_2$]-Mnt composite.

140°C with a peak at about 111°C. TG curve remains unchanged up to about 75°C and then exhibits a mass loss of about 6.0% up to 140°C and has been attributed to loss of interlayer water. At 273°C, the DTA curve shows the first exothermic peak and the TG curve exhibits a mass loss of about 5.5% in the temperature range 210–330°C, which may be due to the oxidation of the organic hydrogen and partial decomposition of the metal complex. Thus, conversion of the octahedral [Ni(den)$_2$]-Mnt [20,25,26] to lower [Ni(den)]-Mnt species takes place. Similar observation was also reported earlier [26]. Comparing the decomposition temperature of the free salt of the metal complex, it reveals that such metal complex, when intercalated into layered Mnt clay, gets an extra thermal stability of about 50°C. This enhanced thermal stability of the metal complex may be due to shielding effect by the alumino-silicate layers structure of the clay. The DTA curve shows the second and third exothermic peaks at 354 and 456°C, respectively. The TG curve does not show any sharp mass loss but exhibits a very small mass loss in the temperature range 350–470°C and may be due to oxidation of the residual carbon left over the clay as charcoal during the oxidation of the den molecule at lower temperature (around 273°C) as well as partial oxidative decomposition of [Ni(den)]-Mnt. The exothermic peak of the DTA curve observed for the composite prepared by the interaction between Ni-Mnt and den reported earlier [26] differs from the above and is perhaps due to difference in packing of the metal complex in the interlamellar spacing and rate of heating the composite. The DTA curve shows the fourth exothermic peak at 557°C, which may be due to oxidation of carbon remained as charcoal on the clay and also oxidative decomposition of the metal complex converting to NiO. The endothermic dehydroxylation peak of Mnt (Fig. 1) expected near 500°C is not observed because it overlaps with the exothermic peak. The TG curve exhibits a mass loss of about 6.0% in the temperature range 500–700°C and may be attributed to the mass loss by oxidation of residual carbon and dehydroxylation of the layered structure of Mnt. The major thermal changes that occur with mass loss of intercalated composite may be presented as:

$$[\mathrm{Ni(den)_2}]\text{-Mnt}.x\mathrm{H_2O} \xrightarrow[\text{Endothermic}]{111^\circ\mathrm{C}} [\mathrm{Ni(den)_2}]\text{-Mnt} + x\mathrm{H_2O} \quad (2)$$

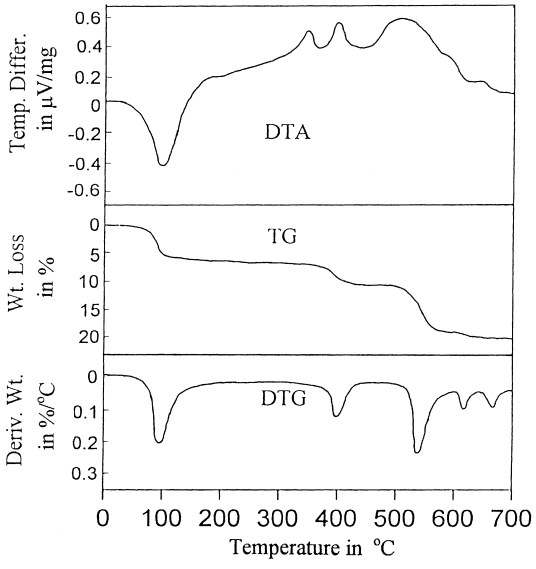

Fig. 3. TG–DTG–DTA curves of $[Ni(tpy)_2]$-Mnt composite.

$$[Ni(den)_2]\text{-Mnt} \xrightarrow[\text{Exothermic}]{273^\circ C} [Ni(den)_{2-x}]\text{-Mnt} + (den)_x \quad (3)$$

$$[Ni(den)_{2-x}]\text{-Mnt} \xrightarrow[\text{Exothermic}]{557^\circ C} [NiO]\text{-Mnt} + \text{other products} \quad (4)$$

The DTA, TG and DTG curves of $[Ni(tpy)_2]$-Mnt composite are shown in Fig. 3. The DTA and TG curves show 5 and 4 peaks, respectively. The DTA curve shows an endothermic peak in the temperature range 50–140°C. The TG curve shows a mass loss of about 6% in the same temperature range and is attributed to loss of water from the inter-layer of the clay matrix. The DTA curve shows the first exothermic peak at about 340°C and the TG curve shows a very little loss of mass in this temperature range indicating some oxidative decomposition of the organic moiety from the metal complex. At about 400°C, the DTA curve shows the second exothermic peak. The TG curve shows a mass loss of about 3.5% in the temperature range 390–410°C, which may be due to the oxidation of the organic hydrogen and partial decomposition of the metal complex. The free salt of the metal complex, i.e., $[Ni(tpy)_2]X_2$ (where X=halide or other anions) [27] are only stable up to about 200°C and above this converts to $[Ni(tpy)]X_2$ by losing one tpy molecule. This clearly indicates that the metal complex gets extra thermal stability by about 150–200°C upon intercalation into interlamellar spacing of the layered Mnt clay. This enhancement of thermal stability is probably due to combined effects of π interaction between the aromatic rings of tpy and the oxygen plane of the alumino-silicate of Mnt [28] as well as the shielding effects of the layered Mnt clay. But in case of $[Ni(den)_2]$-Mnt, the enhancement of the thermal stability is only about 50°C since there is no π interaction between den and the oxygen plane of Mnt. The DTA curve shows the third exothermic peak at 505°C and therefore, the endothermic dehydroxylation peak of Mnt at around 500°C (Fig. 1) is perhaps overlapped with the exothermic peak. The TG curve shows a mass loss of about 8.5% in the temperature range 500–560°C which may be attributed to the conversion of the monoligated metal complex into metal oxide, i.e., NiO with simultaneous oxidative decomposition of the tpy molecule and partial dehydroxylation of the layered clay structure. The fourth and fifth exothermic peaks of the DTA curve occur at about 575 and 645°C, respectively, and the TG curve shows very little mass loss in those temperature range, which may indicate the gradual oxidation of the carbon deposited during oxidative decomposition of the organic moiety on the clay as charcoal. The major thermal changes that occur with mass loss of the intercalated composite may be presented as:

$$[Ni(tpy)_2]\text{-Mnt.}xH_2O \xrightarrow[\text{Endothermic}]{110^\circ C} [Ni(typ)_2]\text{-Mnt} + xH_2O \quad (5)$$

$$[Ni(tpy)_2]\text{-Mnt} \xrightarrow[\text{Exothermic}]{397^\circ C} [Ni(tpy)_{2-x}]\text{-Mnt} + (tpy)_x \quad (6)$$

$$[Ni(tpy)_{2-x}]\text{-Mnt} \xrightarrow[\text{Exothermic}]{505^\circ C} [NiO]\text{-Mnt} + \text{other products} \quad (7)$$

$$[NiO]\text{-Mnt} \xrightarrow[\text{Exothermic}]{574 \text{ and } 643^\circ C} \text{Unknown products} \quad (8)$$

3.2. X-ray diffraction studies

The XRD patterns alongwith basal spacing (d_{001}) data of the intercalated metal-complex-Mnt composites are shown in Fig. 4. It reveals from Fig. 4a that

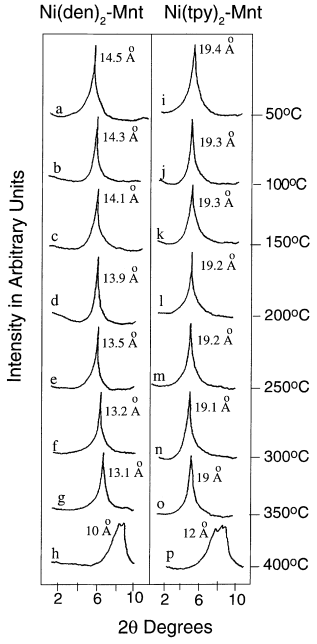

Fig. 4. X-ray diffraction patterns and basal spacing (d_{001}) of oriented samples of intercalated $[Ni(den)_2]$-Mnt (a–h) and $[Ni(tpy)_2]$-Mnt (i–p) composites heated at different temperature (50–400°C) for 1 h in air atmosphere.

the cationic $[Ni(den)_2]^{2+}$ is intercalated into the Mnt clay, because the observed basal spacing, i.e., 14.5 Å of the intercalated composite is slightly more than the summation of the thickness (9.6 Å) of the clay layer and the diameter (about 4.5 Å) of the metal-complex cation [25]. The basal spacing (d_{001}) value gradually decreases as the temperature of drying increases (Fig. 4b–h). The decrease of the basal spacing (d_{001}) from 14.5 to 14.1 Å during heating at 150°C (Fig. 4c) is attributed to loss of water molecules from the interlayer spacing. At about 250°C (Fig. 4e), the basal spacing (d_{001}) is decreased to 13.5 Å which is not adequate to accommodate the octahedral structure of the metal complex in the interlayer spacing and thus may indicate the presence of a slightly distorted octahedral structure. In the temperature range of 300–350°C (Fig. 4f and g), the interlayer spacing was further reduced to about 3.5 Å revealing transformation of the octahedral metal complex into other lower species, possibly to pseudo-octahedral $[Ni(den)]^{2+}$ species [20]. And at about 400°C (Fig. 4h), the interlayer spacing is almost collapsed and shows a basal spacing (d_{001}) of about 10 Å exhibiting multiple XRD peaks which may indicate mixture of different products containing intercalated NiO.

The product obtained from the interaction of bulky octahedral cationic species $[Ni(tpy)_2]^{2+}$ and Mnt shows basal spacing (d_{001}) (Fig. 4i) of about 19.4 Å at 50°C indicating that the cationic species is intercalated into the clay platelets because the summation of the layer thickness (9.6 Å) and dimension (about 9.5 Å) of the metal complex matches well with the observed basal spacing (d_{001}) value, i.e., 19.4 Å. On drying the composite with raising temperature, the basal spacing (d_{001}) decreases slightly to 19.3 Å up to 150°C, which is attributed to loss of water from the interlayer structure. On further raising the temperature up to 350°C, the basal spacing (d_{001}) of the composite gradually reduces to 19.0 Å (Fig. 4o), which may still indicate the presence of the octahedral structure of the $[Ni(tpy)_2]^{2+}$ species in the interlamellar spacing of the layered Mnt clay matching its shape with the hexagonal hollows of the clay surface [29]. But, at about 400°C (Fig. 4p) the basal spacing (d_{001}) value decreases to about 12 Å and exhibiting multiple XRD peaks indicating that the metal complex is decomposed oxidatively to Ni^{2+}/NiO and/or converted into other lower monoligated [27] species like $[Ni(tpy)]^{2+}$ within the interlayer space. It is known that the salt of $[Ni(tpy)_2]^{2+}$ is stable up to 200°C in free state and above it, the metal complex converts to monoterpyridine $Ni(tpy)]^{2+}$ species [27]. Therefore, XRD data reveal that the enhancement of the thermal stability of about 150–200°C is probably due to π interaction [28] between the oxygen plane of Mnt and the aromatic rings of tpy as well as thermal shielding by the clay platelets.

3.3. Infrared spectroscopic studies

FT-IR spectra of Na-Mnt and intercalated composites are shown in Fig. 5. Four major bands are observed at about 3626, 1635, 1040 and 917 cm^{-1} (Fig. 5a) which are due to ν(OH), δ(OH), ν(SiO) and Al-OH-Al deformation bands, respectively, of the alumino-silicate layers of Mnt. The other OH deformations occur near 800 cm^{-1} as very weak bands. The $\nu(CH_2)$ bands at 2920 and 2872 cm^{-1} of the metal complex in $[Ni(den)_2]$-Mnt are observed (Fig. 5b) as weak bands. The $\delta(CH_2)$, $\omega(CH_2)$ and $\omega(NH_2)$ bands at 1447, 1380 and 1336 cm^{-1}, respectively, of the

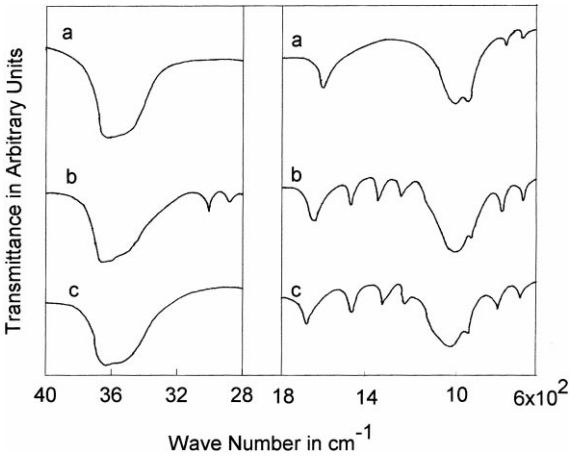

Fig. 5. FT-IR spectra (600–4000 cm^{-1}) of Na-Mnt, [Ni(den)$_2$]-Mnt and [Ni(tpy)$_2$]-Mnt.

metal-complex are observed in the intercalated composites (Fig. 5b). The multiple bands in the region 600–800 cm^{-1} due to $\rho(NH_2)$, skeletal vibration etc. of the free metal complex are not clearly observed, but only two weak bands at 783 and 694 cm^{-1} are found which are difficult to identify. FT-IR spectra (600–1500 cm^{-1}) of the intercalated [Ni(den)$_2$]-Mnt composite heated at different temperatures are shown in Fig. 6a–e. Up to about 250°C, the intensity of the characteristic bands of the metal complex remain almost unchanged. The formation of H-bond between N–H group of the ligand moiety of the metal complex and oxygen-plane of Mnt is likely and may be one of the reasons for the enhancement of thermal stability of the composite. The intensities of the characteristic bands(Fig. 6d) of the metal complex at about 350°C are considerably reduced indicating oxidative decomposition of the metal complex into other lower species. Similarly, the $\nu(CH_2)$ bands at 2920 and 2872 cm^{-1} (Fig. 5b) of the composite are stable up to 250°C, but at about 350°C, the intensity of the bands are reduced to minimum. At about 400°C, the characteristic bands of the metal complex are almost vanished and thus indicating complete decomposition of the metal complex.

The ring stretching (C–H in-plane ring stretching vibration) occurring below 1500 cm^{-1} are observed in the [Ni(tpy)$_2$]-Mnt composite (Fig. 5c) as distinct bands. The C–H out-of-plane deformation vibrations of the heterocyclic tpy rings in the region 650–800 cm^{-1} are also observed as distinct bands in the

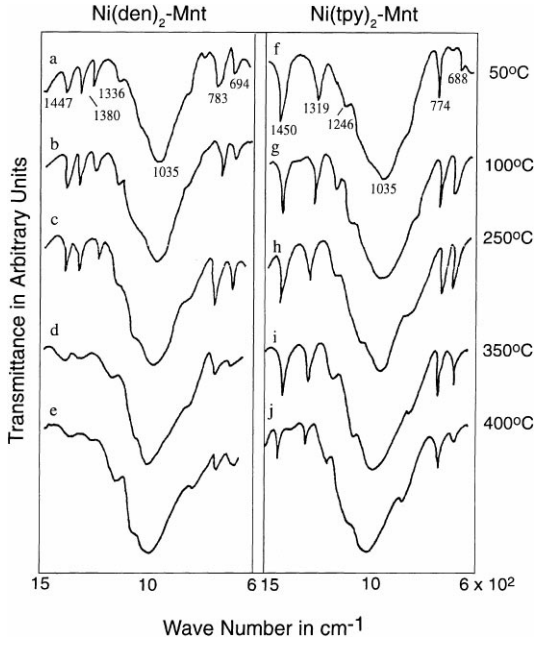

Fig. 6. FT-IR spectra (600–1500 cm^{-1}) of the intercalated [Ni(den)$_2$]-Mnt (a–e) and [Ni(tpy)$_2$]-Mnt (f–j) composites heated at different temperature (50–400°C) for 1 h in air atmosphere.

intercalated composite (Fig. 5c). As the intercalated composite is heated, the band near 1635 cm^{-1} at room temperature due to δ(OH) gradually shifts to lower wave number up to 1604 cm^{-1} at about 400°C. This shift may be an indication that some π interaction between the aromatic tpy and oxygen plane of Mnt occurs. The FT-IR (600–1500 cm^{-1}) spectra of [Ni(tpy)$_2$]-Mnt composite heated at different temperatures are shown in Fig. 6. The peak positions and intensities of the characteristic bands of the metal complex in the intercalated composite remain unchanged up to about 350°C (Fig. 6i) indicating stable state of the metal complex in the interlamellar spacing. At about 400°C, the intensities of the characteristic bands of the metal complex in the intercalated composite are considerably reduced indicating oxidative decomposition and transformation of the octahedral metal complex into other forms.

4. Conclusions

Thermal stability of the intercalated [Ni{Di(2-aminoethyl)amine}$_2$]-Montmorillonite (**I**) and [Ni(2,2′:

6′,2″terpyridine)$_2$]-Montmorillonite (**II**) composites, studied by thermal(TG, DTA, DTG) analyses substantiated by XRD and IR spectroscopy, are about 50 and 150°C higher compared to melting/decomposition of their respective free metal complex salts. Metal complex with aromatic backboned ligands gets higher thermal stability than that containing aliphatic one upon intercalation into Mnt and this may be due to π interactions between the oxygen-plane of Mnt and the aromatic rings of tpy while there is no π interaction between the oxygen-plane of Mnt and den. XRD data show that the basal spacing (d_{001}) of the **I** composite, i.e., 14.5 Å at 50°C show a gradual decrease on increasing the temperature and reached a value of about 13.5 Å at 250°C. This corresponds to a distorted octahedral intercalated complex in the interlamellar spacing. On the other hand, the **II** composite shows a basal spacing (d_{001}) of 19.4 Å at 50°C and decreases slightly to 19.0 Å at about 350°C indicating presence of octahedral metal complex in the interlamellar spacing and thus the XRD data corroborate the observation made by the thermal analyses. The characteristic bands of IR spectra of the composites **I** and **II** in the temperature range 50–400°C also show that these are stable up to about 250 and 350°C, respectively, and thus corroborate the data of thermal as well as XRD analyses. Such metal-complex-clay composites may be utilized for developing microporous layered materials exhibiting comparatively higher thermal stability.

Acknowledgements

The authors are grateful to the Director, RRL Jorhat, for encouragement and permission to publish the paper. Thanks are also due to Dr. P.C. Borthakur, Head, Material Science Division, RRL Jorhat, for his keen interest and support. The authors also thank Prof. A.T. Baker, University of Technology, Sydney, Australia, for providing the metal-complex and crystallographic data.

References

[1] R.M. Barrer, J. Inclusion Phen 4 (1986) 109.
[2] R.M. Barrer, Pure & Appl. Chem. 61 (1989) 1903.
[3] R.M. Barrer, K. Brummer, Trans. Faraday Soc. 59 (1963) 959.
[4] E. Booij, J.T. Kloprogge, J.A. Rob van Veen, Appl. Clay Sc. 11 (1996) 155.
[5] J.E. Mark, Y.C. Lee, P.A. Bianconi, Hybrid organic-Inorganic composites, ACS Symp. Ser. 585, Am. Chem. Soc., Washington DC, 1995. pp.378–392.
[6] B.K.G. Theng, The Chemistry of Clay-organic Reactions, 1st Edition, Wiley, New York, Toronto, 1974, Chapter 1.
[7] M.B. McBride, M.M. Mortland, Clays Clay Miner. 21 (1973) 323.
[8] D.E.W. Vaughan, in: W. H. Frank, T. E. Whyte (Eds.), Recent development in pillared interlayered clays: perspective in molecular sieve science, ACS Symposium Series 368, 1980, p. 308.
[9] H. Favre, G. Lagaly, Clay Miner. 26 (1991) 19.
[10] H. Lao, S. Latieule, C. Detellier, Chem. Mater. (1991) 1009.
[11] H. Lao, C. Detellier, Clays Clay Miner. 42 (1994) 477.
[12] T.J. Pinnavaia, Science 220 (1983) 365.
[13] V.J. Thielmann, J.L. McAtee Jr., J. Chromatog. 105 (1975) 115.
[14] R.M. Barrer, D.L. Jones, J. Chem. Soc. A (1971) 2594.
[15] R.H. Loeppert, M. M Mortland, T.J. Pinnavaia, Clays Clay Miner. 27 (1979) 201.
[16] M. Bora, D.K. Dutta, in: S.C. Lahiri, P. Chakraborty (Eds.), Proc. 32nd Annul. Conv. Chem., Rajasthan, India, 1995, Abs. No. ING(OP)-5.
[17] M. Bora, J.N. Ganguli, D.K. Dutta, in: S.N. Gupta (Ed.), Proc. 33rd Annul. Conv. Chem., Coimbatore, India, 1996, Abs. No. IND-27.
[18] J.E. Gillott, Clay in Engineering Geology, 1st Edition, Elsevier publishing company, 1968, Chapter 11.
[19] A.B. Searle, R.W. Grimshaw, The Chemistry and Physics of Clays and Other Ceramic Materials, Ernest Benn, London, 3rd Edition, 1960, Chapter 5.
[20] N.F. Curtis, H.K.J. Powell, J. Chem. Soc. A (1968) 3069.
[21] A.T. Baker, D.C. Craig, A.D. Rae, Aust. J. Chem. 48 (1995) 1373.
[22] G. W. Brindley, G. Brown, Crystal structure of clay minerals and their X-ray identification (Mineralogical Society, Monographs No. 5), London, 1984, Chapter 5.
[23] R.E. Grim, Clay Mineralogy, McGraw-Hill, New York, 1953, Chapter 9.
[24] V.C. Farmer, in: V.C. Farmer (Ed.), The Layered Silicates: the Infrared Spectra of Minerals, Mineralogical Society Monograph 4, 1974, p. 331.
[25] S. Biagini, M. Cannas, J. Chem. Soc. A (1970) 2398.
[26] W. Bodenheimer, L. Heller, B. Kirson, S. Yariv, Israel J. Chem. 1 (1963) 391.
[27] R. Hogg, R.G. Wilkins, J. Chem. Soc. (1962) 341.
[28] S. Yariv, M. Müller-Vonmoos, G. Hahr, A. Rub, Thermochim. Acta 148 (1989) 457.
[29] J. Breu, C.R.A. Catlow, Inorg. Chem. 34 (1995) 4504.